Dynamical effects of interactions and the Tully-Fisher relation for Hickson compact groups

C. Mendes de Oliveira [1,2,3], P. Amram [4], H. Plana [5]
and
C. Balkowski [6]
oliveira@astro.iag.usp.br

ABSTRACT

We investigate the properties of the B-band Tully-Fisher (T-F) relation for 25 compact group galaxies, using $V_{\rm max}$ derived from 2-D velocity maps. Our main result is that the majority of the Hickson Compact Group galaxies lie on the T-F relation. However, about 20% of the galaxies, including the lowest-mass systems, have higher B luminosities for a given mass, or alternatively, a mass which is too low for their luminosities. We favour a scenario in which outliers have been brightened due to either enhanced star formation or merging. Alternatively, the T-F outliers may have undergone truncation of their dark halo due to interactions. It is possible that in some cases, both effects contribute. The fact that the B-band T-F relation is similar for compact group and field galaxies tells us that these galaxies show common mass-to-size relations and that the halos of compact group galaxies have not been significantly stripped inside R_{25}.

We find that 75% of the compact group galaxies studied (22 out of 29) have highly peculiar velocity fields. Nevertheless, a careful choice of inclination, position angle and center, obtained from the velocity field, and an average of the velocities over a large sector of the galaxy enabled the determination of fairly well-behaved rotation curves for the galaxies. However, two of the compact group galaxies which are the most massive members in M51–like pairs, HCG 91a and HCG 96a, have very asymmetric rotation curves, with one arm rising and the other one falling, indicating, most probably, a recent perturbation by the small close companions.

Subject headings: Galaxies: individual (galaxies: kinematics and dynamics — galaxies: interactions — galaxies: ISM — galaxies: intergalactic medium — instrumentation: interferometers)

1. Introduction

The influence of environmental effects on the internal dynamics and matter distribution of compact group galaxies has not yet been clearly established, mostly due to lack of reliable kinematic data. A recent study of the internal kinematics of 30 galaxies by Nishiura et al. (2000, hereafter N2000) found that asymmetric and peculiar rotation curves are more frequently seen in the Hickson Compact Groups (HCG) spiral galaxies than in field or cluster spirals and the dynamical properties of the galaxies do not seem to correlate with any group or galaxy parameter. An older but very influential study is that by Rubin et al. (1991,

[1]Universidade de São Paulo, IAG, Departamento de Astronomia, Rua do Matão 1226, 05508-900, São Paulo, SP, Brazil

[2]Max-Planck-Institut für Extraterrestrische Physik, Giessenbachstrasse, D-85748 Garching b. München, Germany

[3]Universitäts-Sternwarte der LMU, Scheinerstrasse 1, D-81679 München, Germany

[4]Observatoire Astronomique Marseille-Provence & Laboratoire d'Astrophysique de Marseille, 2 Place Le Verrier, 13248 Marseille Cedex 04, France

[5]Universidade Estadual de Santa Cruz, Dept. Ciencias Exatas e Tecnologicas, Rodovia Ilheus-Itabuna, km. 16, 45650-000, Ilhéus, BA, Brazil

[6]Observatoire de Paris, GEPI, CNRS and Universite Paris 7, 5 Place Jules Janssen, F-92195 Meudon Cedex, France

hereafter R1991), who analyzed rotation curves for 32 Hickson compact group galaxies and found that 2/3 of them had peculiar rotation curves. For the subsample of galaxies for which rotation curves were possible to be derived, they found a large offset of the T-F relation with respect to the field relation in the sense that galaxies in compact groups have "too low velocities for their luminosities or, alternatively, luminosities which are overbright for their rotation velocities." This suggested to the authors that spiral galaxies in compact groups have low mass-to-light ratios compared to field galaxies by about 30% which, in turn, could be explained if compact group galaxies have smaller dark halos than their field counterparts. Given that compact groups are environments where tidal encounters are common, it may be expected that interactions have stripped or disrupted the galaxy dark halos at some level. These conclusions have important consequences for the determination of group lifetimes and understanding how compact groups evolve and eventually merge.

We revisit this important problem using a new dataset for 25 galaxies, of which 13 are in common with either the sample of R1991 or N2000 or both. In this paper we re-examine the T-F relation for compact group galaxies. Our study differs from the previous work in that it uses rotation curves obtained from 2-dimensional velocity fields. In a number of cases this allows a more accurate determination of the rotation curves than was possible with slit spectroscopy. Additionally, a fuller characterization of the kinematics of each galaxy is possible. We show that, with these new data, the T-F relation for compact group galaxies is similar to that for galaxies in less dense environments. The exceptions to this conclusion are seen for some of the least massive galaxies in our sample.

This paper is organized as follows. In Section 2 we present the set of rotation curves that are used. In Section 3 we illustrate and discuss comparisons of rotation curves for several galaxies in common with R1991 and N2000 and we show that 2-D spectroscopy is needed if one wants to accurately describe the kinematics of interacting galaxies. Sections 4 and 5 show the results on the T-F relation and a discussion respectively.

2. Data

The data used in this paper are gathered from three publications which studied the kinematics of galaxies in nine compact groups (HCG 10, 16, 19, 87, 88, 89, 90, 91, 96, 100). A detailed description of the observations and data reduction can be found in Mendes de Oliveira et al. (1998), Plana et al. (2003) and Amram et al. (2003). In summary, our dataset consists of Hα emission-line velocity maps obtained with a Fabry-Perot system, from which rotation curves were obtained. For the T-F study we excluded from the sample all the elliptical galaxies. We also excluded galaxies HCG 10a, 10c, 16d and 100a because their rotation curves have a very short extension, well short of R_{25} and galaxies HCG 16b and HCG 100b due to their extremely peculiar rotation curves. We included HCG 19a in our sample, although Hickson (1993) classifies it as an E2 galaxy, because we have reclassified it as an S0 based on its kinematic properties. In addition, we included in our sample unpublished data for two other galaxies (HCG 07c and HCG 79d).

We show in Figs. 1a and 1b the rotation curves for the galaxies in the sample studied in this paper. The x-axis plots r/R_{25}, the galaxy radius along its major axis normalized by R_{25}, the length of the major axis at the 25 mag arcsec^{-2} isophote (as given by Hickson 1993; note, however that in Plana et al. 2003 and Amram et al. 2003, the value for R_{25} was taken from de Vaucouleurs et al. 1991, the RC3, resulting in slightly different numbers from those used here). In order to obtain a V_{max} for use in the T-F relation (represented by a black dot in each subpannel of Figs. 1a and 1b) we have computed the maximum velocity of the average velocity curve (single average of the values for the receding and approaching sides). V_{max} is not the best kinematic parameter to be used in the T-F relation, since V_{flat}, the velocity of the flat portion of the curve or V_{2d}, the velocity at two times the galaxy scale length are known to yield less scatter in the T-F relation. However, the use of V_{max} allowed us to use the largest possible number of compact group galaxies.

The control sample used for the T-F comparison was the sample of Sb and Sc galaxies from Courteau (1997), where we used their "Vmax" as the equivalent to the maximum velocity deter-

mined by us. We also used the sample of galaxies in the Ursa Major cluster (Verheijen 2001), in order to fill in the lower end of the mass sequence in the T-F diagram. We note that our values of V_{max} are adjusted by the cosmological correction (1+z) as are also the values given for the galaxies in the control samples. All velocities were corrected for the same Virgocentric infall (Paturel et al. 1997) when distances were obtained using the Hubble law (for our sample and Courteau's sample).

We note that in Fig. 1 the rotation of HCG 87a is one-sided because half of this almost edge-on galaxy is not observed due to a strong dust lane.

3. Comparisons with previous long-slit spectroscopy

The 2-D velocity maps obtained with a Fabry-Perot instrument allowed us to mimic a slit through our data in order to recover the rotation curves obtained from long-slit spectroscopy. In this way, we could make a direct comparison with previous rotation curves obtained by other authors in order to investigate the reason for existing differences in the shapes and amplitudes of the rotation curves between different studies, for a given galaxy.

We give an example in Fig. 2, where it is clear why with long-slit spectroscopy the derived rotation curves do not always correspond to the overall kinematics of the galaxies. The rotation curve derived by R1991 for HCG 88a (reproduced in Fig. 2) shows asymmetries with disagreement between the two sides of the galaxy (a bifurcation of the curve at a radius of 10 arcsec). We overplot on Fig. 2 the Fabry-Perot data for HCG 88a, with values restricted to a narrow cone around the galaxy major axis (to mimic a slit), using the particular values of center, inclination and position angle derived by R1991 photometrically. Inspecting the figure we see that for radii larger than 10 arcsec, there is good agreement between the slit-spectroscopy and Fabry-Perot data, if the photometrically derived center, inclination and position angle are used. However, the overall shape of the curve changes when such parameters are derived from the velocity map and a large sector of the galaxy is averaged (the resulting rotation curve is shown in Plana et al. 2003 and in Fig. 1). In particular, if the kinematic parameters are used and velocities over a large sector of the galaxies are averaged, the bifurcation present in Fig. 2, at r $\sim$ 10 arcsec, disappears, and the galaxy has normal kinematics, with both sides of the curve matching.

In order to understand the magnitude of the variations of the parameters measured from the kinematic and photometric data we list in Table 2 values for the inclination, PA and differences between centers measured from the continuum images and velocity fields. Detailed discussion on the method used to obtain the center, PA of the major axis, and inclination of the galaxies are given in Amram et al. (1996). We included in the table not only the galaxies used in the Tully-Fisher relation but also those that were considered too peculiar or for which the gas extension was too short. We list in the last four columns the values of inclination and PA given by R1991 and N2000, when available.

A comparison of the inclinations derived from the Fabry-Perot map and from the continuum images was done by subtracting columns 2 and 3 of Table 2 (and normalized to one of the two). The differences spread approximately around zero, with an rms of 20% (for the galaxies used in the Tully-Fisher relation). This indicates that there is no systematic error introduced in the determination of the maximum velocities due to the measurement of the inclination from either photometric or kinematic data. However, a similar comparison with the smaller subsample in common with R1991 and N2000 show a slight overestimate of the inclinations obtained by these authors, as compared to our estimates. This would indicate that the V_{max} derived by them would be expected to be lower on average than those obtained by us (and in fact, the values of V_{max} derived by R1991 in particular tend to be lower than those derived in our study).

A comparison between columns 4 and 5 of Table 2, of the kinematic and photometric PA's for the galaxies used in the T-F analysis, shows that about 1/3 of the galaxies have misalignments (greater than 10 degrees) between the kinematic and photometric axes. This may be an indication that the gas is not in equilibrium in these galaxies (HCG 10d, 16c, 19a, 88b, 89d, 91a, 91c, 96a). If that is the case, and for an example the gas is collapsing and/or there is additional dispersion, then

the V_{max} we compute using the rotation curve of the gas is a lower limit to the real V_{max} (indicated by the total mass). In other words, the real mass of the galaxy would then be higher than what we infer from our measurements. We note that four of the six galaxies that were too peculiar or had too short gas extensions to enter the T-F analysis also present misalignments between the kinematic and photometric axes (HCG 16b, 16d, 10c, 100b).

Similar results are obtained when comparing the kinematic PA's to the corresponding photometric values derived from either R1991 and/or N2000 for the smaller subsample of galaxies in common (comparing columns 4 and 8 and columns 4 and 10 of Table 2).

We are not able to make a direct comparison between the centers we measure with those measured by R1991 and/or N2000 since we do not know the exact value they used (this problem is related to the fact that we do not have information from our Fabry-Perot data about the systemic velocities of the galaxies, given the scanning nature of the instrument, Amram et al. 1992, and also related to the fact that we do not know exactly where they positioned the slits). We then list in column 6 of Table 2 only the difference in arcsec between the measured kinematic and photometric center. The center of the continuum image was taken as the point of maximum intensity. The center of the velocity field was chosen to be a point along the major axis which made the rotation curve symmetric or as symmetric as possible (with similar amplitudes for the receding and approaching sides). This freedom with the Fabry-Perot data was, in fact, one reason why it was possible to construct fairly well behaved rotation curves even when the velocity maps were highly peculiar due to localized non-circular motions. The values for $|\Delta_{kin-cont}|$ varied from zero to six arcseconds.

Our conclusion is that the velocity fields of compact group galaxies are, in several cases, significantly affected by non-circular motions, local asymmetries and misalignments between the kinematic and stellar axes. A fine tuning of map parameters (center, inclination and position angle of the velocity fields) and an average of the velocities over a large sector of the galaxy are needed to derive reliable rotation curves and representative values of V_{max}.

A few other comparisons with data from R1991 and N2000 are exemplified in Fig. 3. In all cases we plot rotation curves resulting from a cut through the Fabry-Perot data, using the parameters given by the author's (photometric parameters). An important point becomes clear when inspecting Fig. 3, especially Figs. 3a, 3b and 3f. In these cases the rotation curves derived from the 2-D maps extend beyond the long-slit ones, which is also another reason for the discrepant values of derived V_{max}, using these two different techniques, Fabry-Perot or long-slit. We should have in mind, however, that an over/underestimation of the inclination leads to an over/underestimation of the extension of the rotation curves.

Another point we should note is that the rotation curves derived by Fabry-Perot spectroscopy are much more well behaved in the sense that more often the two sides of the curves approximately agree and they are either flat or rising in the last measured point. In fact, we have no example of galaxy with a rotation curve that drops in both sides as one would expect in the Keplerian case.

4. Results

Table 1 summarizes the main parameters for each galaxy. In columns (1) and (2) we show the identification and length of semi-major axis of the galaxy as given by Hickson (1993). The morphological classification for the galaxies taken from Hickson (1993) and from NED are given in columns (3) and (4) respectively . The values for the total B magnitudes of the galaxies, listed in column (5), B_{Tcor}, were obtained from the B_T listed in Hickson et al. (1989), corrected by galactic extinction (Schlegel et al. 1998) and by the extinction due to inclination (Tully et al. 1998). The same corrections were also applied to the magnitudes of the galaxies in the control samples. The velocities listed in (6) are the maximum rotational velocities obtained from the average velocity curves as shown in Fig. 1. In (7) we list vvir, the heliocentric radial velocity of the galaxy, corrected for the local group infall onto Virgo, from the Hyperleda database. The absolute magnitudes in column (8) were obtained from $M = B_{Tcor} - 5 * LG(vvir/75)$. Finally, in column (9) we marked with a P those galaxies whose velocity fields were considered highly disturbed either by Amram et al. (2003), Plana et al. (2003)

or Mendes de Oliveira et al. (1998).

The morphological types are represented in the sample in the following proportion $S0 : Sa : Sb : Sc : Sd : Sm : I$=1:2:3:12:3:2:2, with preponderance of the Sc and Scd types (both counted in the Sc bin). We note that two galaxies, HCG 16c and HCG 96d, were classified as "irregular" by Hickson (1993), indicating that they had peculiar morphologies and not that they are truly irregular galaxies. The magnitudes of the galaxies ranged from $M_B \sim$ –18.0 to –22.0 + 5 log h_{75}.

We show in Fig. 4 the T-F relation in the B band for the Hickson compact group galaxies, for the Sb and Sc galaxies in the lower density environments studied by Courteau (1997), and for Sb-Sd galaxies in the Ursa Major cluster studied by Verheijen (2001). The R magnitudes given in Courteau (1996) were transformed to the B magnitudes using the observational relation between morphological type index and the $B - R$ colors (de Jong 1996). The solid line in Fig. 4 represents a linear-squares fit to the Courteau's data (M_B = –7.05 log (V_{max}) – 4.57). The broken lines indicate the ± one sigma dispersion (rms=0.63) for their data. The dispersion for the HCG galaxies around the solid line is rms=0.82 for the whole sample of 25 galaxies and rms=0.65 (similar to that for the control sample of Courteau 1997) if the outliers HCG 89d, 91c, 96c, 96d are not considered (see section 5.1 for the discussion why these galaxies could have a peculiar location in the T-F relation). The sample of Verheijen (2001) for the Ursa Major cluster spirals presents a *smaller* dispersion around the solid line of rms=0.43, as expected for *cluster* galaxies.

Our main result is that galaxies in compact groups follow the T-F relation, with a few exceptions. This result is in contrast with an earlier result by R1991, who found an offset of the T-F relation for most galaxies in compact groups in the sense that galaxies in compact groups have lower velocities for a given luminosity. The disagreement is explained by the differences in the amplitudes of the derived rotation curves, V_{max}, as discussed in Section 3, mainly due to a different choice of galactic parameters (center, inclination and position angle) and a less extended rotation curve in the case of curves obtained from long-slit spectroscopy. Generally, a choice of parameters guided by photometry alone (when no kinematic maps are available) will result in a lower V_{max} of a galaxy, affecting the T-F relation in the direction of the R1991 result.

5. Discussion and future prospects

The fact that the B-band T-F relation is similar for compact group and field galaxies tells us that these galaxies show common mass-to-size relations. However, since the parameters for the T-F relation are mostly derived in the inner parts of the galaxy, this agreement does not tell us much about the dark matter, a dominant component in the *outer* parts (although for the latest-type galaxies we do expect a significant contribution of the dark component in the inner regions as well, Blais-Ouellette et al. 1999). Since the internal velocity dispersions of the compact group galaxy members (250 km s^{-1}) are of the same order of their orbital velocities, interactions in the compact-group environment are likely to lead to mergers. In fact, N-body simulations of compact group formation and evolution (Barnes 1989) show that the fate of a compact group is merging in a few crossing times. In order to avoid fast merging, the theoretical expectation is that the compact group environment should change the shapes of the dark matter halos of galaxies that traverse the group, specifically by transforming the single-galaxy halos in a common halo around the group (e.g. Athanassoula, Makino & Bosma, 1997). Our observations cannot test (directly) this hypothesis but do show that the galaxy halos have not been significantly stripped inside R_{25}. Nevertheless, mass models using a common halo for the groups added to the individual star distributions of each galaxy should be performed to test this scenario.

5.1. The outliers of the Tully-Fisher relation

It is clear from Fig. 4 that a few of the lowest-mass members of compact groups lie well "above" the relationship. If they once had the T-F parameters similar to galaxies in less dense environment, they could have either brightened by 1 to 2 magnitudes in the B band, to get to their present position, they could have lost a substantial amount of mass, or they could have undergone a combination of these processes.

A natural way that the smaller members could

have brightened is by forming stars, induced by the interactions the galaxy may have suffered within the group. For a given rate of star formation, the brightening of a galaxy will be much more noticeable for a low-mass than for a high-mass galaxy. As an example, for a large spiral galaxy with mass of 10^{11} solar masses, an episode of star formation that generates, say, 10 solar masses per year, would increase the luminosity of the galaxy in the B band only by about 20%, while for a galaxy with a mass ten times lower, the same episode of star formation would triple the luminosity of the galaxy, enhancing its magnitude by 1.2 mag. Moreover, the two galaxies in the lowest-mass end of the diagram (HCG 89d and 96d) may have large quantities of gas, given their late morphological types. In fact, for HCG 96d, for which a study of HI has been made by Verdes Montenegro et al. (1997), the HI gas contributes with half of the total mass. HCG 89d and HCG 96d have masses (obtained from their maximum velocities inside R_{25} and the virial theorem) well below 10^{10} solar masses and their colours are quite blue (B–R=0.8 and 0.97 respectively, Hickson 1993 and Verdes-Montenegro et al. 1997). It is therefore quite probable that HCG 89d and HCG 96d are "above" the T-F relation mainly due to brightening caused by star formation.

HCG 96c, which may deviate from the T-F relation for similar reasons, is the least massive galaxy in an M51-like pair (with the Seyfert galaxy HCG 96a). HCG 96c is noted by Laurikainen and Moles (1988) as the galaxy with the highest star-formation rate per unit area among interacting galaxies. Its colours (B-V)=0.95 and (U-B)=0.38 are consistent with this scenario (Laurikainen and Moles 1988).

Another galaxy that lies "above" the T-F relation is HCG 91c, which has a colour of B–R=1.08 (Hickson 1993) and a mass inside R_{25} of 2.5×10^{10} M$\odot$. This galaxy clearly shows two dynamic components with quite similar rotation curves (plotted in Fig. 1 as C1 and C2, also see Amram et al. 2003). There are two points we would like to make about this galaxy. First, given the double kinematic component, we strongly suspect that this galaxy is probably the result of a merger of two similar-mass galaxies although we have no signs of this in the photometric profile of the object. In the T-F relation plotted in Fig. 4 we chose to represent this galaxy with the V_{max} of the C1 component and the total B luminosity of the system as a whole. We, therefore, expect, in a naive scenario, that the galaxy will be higher in the T-F relation by at least 0.75 magnitudes, in addition to the amount of brightening due to star formation, if there is any, which, in turn, would explain why this galaxy lies above the T-F relation. The second point, which is related to the first, is that given our arbitrary choice to use only one component (C1) to represent a galaxy which clearly has two equally important kinematic structures, V_{max} for HCG 91c is most probably an underestimate in Fig. 4 and a correction for this would then move the galaxy towards the T-F mean line.

A second mechanism to leave the outliers in the position where they are in the T-F relation would be by mass loss, within R_{25}. This could be caused, for example by disruption or ablation of a part of the dark halo due to strong interactions in the group. If the galaxy loses mass, in first approximation it would move to the left of the diagram. We then calculated how much mass the outliers had to lose in order to move from the position they should have (to lie on the T-F relation) to their actual position in the diagram, if mass-loss alone were acting. The answer is an impossible number – 300-500% of the total mass – making this mechanism very unlikely. We then conclude that the reason why the low-mass galaxies are off the T-F relation is most probably due to enhanced star formation and not mass loss but could be a combination of both. Two galaxies which may have suffered truncation are HCG 89d and HCG 96d, the most deviant galaxies from the T-F relation, which have morphological types Sm and Im respectively. Given their late morphological types we suspect that they contain a significant contribution from a dark component even in their inner regions, although detailed modelling has to be done to check this possibility. Their position in the T-F diagram could, then, be the result of a stripping of this inner dark halo combined with brightening of the galaxy due to star formation (given their blue colors).

A trend of overbright galaxies for their mass was seen, at the low-mass end of the relation, when the T-F diagram of binary galaxies was plotted by Márquez et al. (2002). Three of the least massive galaxies in interacting pairs showed a deviation of

the T-F relation in the same sense as observed by us for galaxies in compact groups. Moreover, Kannappan et al. (2002), studying a sample of bright nearby galaxies brighter than $M_R = -18$, noted that interacting galaxies systematically lied above while Sa galaxies fell below the T-F relation. In fact, they proposed that there is a correlation of the residuals of the T-F relation with the star formation history of the galaxy and when a second parameter such as colour or equivalent width of Hα is taken into account, the scatter on the T-F relation is significantly diminished.

Note that the lowest-mass HCG members deviate from the T-F relation in the opposite sense of those gas-rich galaxies studied by McGaugh et al. (2000) for which a "baryonic correction" (to take into account the gas mass into the "luminosity" of the galaxy) was necessary.

5.2. Fraction of HCG galaxies with peculiar velocity fields

In the last column of Table 1 we marked with a *P* the galaxies whose velocity fields were considered highly disturbed either by Amram et al. (2003), Plana et al. (2003) or Mendes de Oliveira et al. (1998). A total of 17 from 24 galaxies (all in Table 1 but HCG 87a, which could not be classified) are marked peculiar. If we add to this sample those that were not included in the Tully-Fisher analysis because of their strong peculiarities or short gas extension, we find that 22 out of 29 galaxies, or 75% of the sample of studied galaxies have highly disturbed velocity fields. With this high rate of peculiar kinematics, it is striking that the corresponding rotation curves were possible to be obtained and that, on average, galaxies in compact groups follow the T-F relation.

5.3. Asymmetric rotation curves

We can see in Fig. 1 that the rotation curves of HCG 91a (NGC 7214) and HCG96a (NGC 7674) present strong asymmetries, with one arm rising and the other one falling. Both HCG 91a and HCG 96a are the most massive members in M51-like pairs and they are also known to be Seyfert galaxies. We have checked the rotation curves of other most-massive galaxies in M51-like pairs in the sample of Márquez et al. (2002) and we have found several examples of similar rotation curves: NGC 3395/3396, NGC 5395/5394 and NGC 5774/5775. In fact, most galaxies in pairs of galaxies of unequal mass seem to have rotation curves with either one side rising and the other one falling or both falling. Examples of the latter class are NGC 4496a/4496b and NGC 2535/2536 (Amram et al. 1989). Other binary galaxies from Márquez' sample show a rotation curve with high scatter and a trend for asymmetry (e.g. NGC 3769/3769A). Such rotation curves are rare among isolated galaxies. On the other hand, some rotation curves of galaxies of nearly-equal mass (e.g. NGC 5257/5258, Fuentes-Carrera 2003) curiously do not seem to show such peculiarities, presenting more symmetric rotation curves.

If there was mass stripping from a galaxy and if the system had time to relax, then, the potential should be axisymmetric and both sides of the rotation curve should fall. We observe no such rotation curves among compact group galaxies. However, if the interaction is very recent and the system did not have time to relax, the potential could be non-axisymmetric (triaxial) and the resulting rotation curve could have the observed shape. Another possibility is that the halo could be just shaken (not stripped), in which case we would also expect to observe non-axisymmetric rotation curves such as those we observe among compact group galaxies. More N-body simulations are necessary to further clarify these issues.

The prospects for the future are (1) to use near-infrared imaging to check this result, (2) combine rotation curves with surface brightness profiles to model what role the dark matter plays in the mass distribution, specially to detect galaxies that are dominated by dark matter in their central parts, if there are any and (3) to use other more external (to the group) test-particles to test the halo properties at larger radii (e.g. planetary nebula, globular clusters and/or dwarf galaxies). Finally, a detailed comparison of the results presented in this paper with tidal stripping of dark matter halos in cosmological N-body simulations of compact groups would be of great interest.

CMdO deeply acknowledges the funding and hospitality of the Max Planck für Extraterrestrische Physik and the Universitaets-Sternwarte der Ludwig-Maximilians-Universität, where this work was finalized. CMdO would also like to thank the Brazilian FAPESP (projeto temático

01/07342-7), the PICS program for financial support of two visits to the Observatoire de Marseille and Paris/Meudon and the Brazilian PRONEX program. H.P. acknowledges financial support of Brazilian Cnpq under contract 150089/98-8. The authors thank J. Boulesteix and J.L. Gach for helping during the observations and Mike Bolte for very useful comments on the manuscript. We made use of the Hyperleda database and the NASA/IPAC Extragalactic Database (NED). The latter is operated by the Jet Propulsion Laboratory, California Institute of Technology, under contract with NASA.

REFERENCES

Athanassoula, E., Makino, J. & Bosma, A., 1997, MNRAS, 286, 825

Amram, P., Le Coarer, E., Marcelin, M., Balkowski, C., Sullivan, W.T., III, Cayatte, V., 1992, A&AS, 94, 175.

Amram, P., Balkowski, C., Boulesteix, J., Cayatte, V., Marcelin, M., & Sullivan, W. T., III. 1996, A&A, 310, 737

Amram P., Plana H., Mendes de Oliveira C., Balkowski C., Boulesteix J., 2003, A&A, 402, 865

Amram P., Marcelin M., Boulesteix J., Le Coarer E., 1989, A&A Supplement series, 81, 59

Barnes J., 1989, Nature, 338, 123

Blais-Ouellette S., Carignan C., Amram P., Ct S., 1999, AJ, 118, 2123

Courteau S., 1996, ApJS, 103, 363

Courteau S., 1997, AJ, 114, 2402

de Jong R.S, 1996, A&A Supplement series, 118, 557

de Vaucouleurs, G., de Vaucouleurs, A., Corwin, H. G., Buta, J., Paturel, G. and Fouqué, P., 1991, *Third Reference Catalogue of Bright Galaxies*, Springer Verlag (RC3)

Fuentes-Carrera, I., Ph.D. Thesis, 2003.

Hickson P., Kindl E., Auman J. 1989, ApJS, 70, 687

Hickson P. 1993, Astroph.Letter & Comm. 29, 1

Kannappan, S.J., Fabricant, D.G. and Franx, M., 2002, ApJ, 123, 2358.

Márquez, I., Masegosa, J., Moles, M., Varela, J., Bettoni, D., Galletta, G., 2002, A&A, 393, 389.

McGaugh S.S., Schombert J.M., Bothun G.D., de Blok W.J.G., 2000, ApJ, 533, L99

Mendes de Oliveira C., Plana H., Amram P., Balkowski C., Boulesteix J. 1998, ApJ, 507, 691

Nishiura S., Shimada M., Ohyama Y., Murayama T., Taniguchi Y. 2000, AJ, 120, 169 (N2000)

Paturel G., Gouguenheim L., Lanoix P., Marthinet M., Petit C., Rousseau J., Theureau G., Vauglin I. 1997, A&ASS, 124, 109

Plana H., Mendes de Oliveira C., Amram P., Boulesteix J., 1998, AJ, 116, 2123

Plana H., Amram P., Mendes de Oliveira C., Balkowski C., Boulesteix J., 2003, AJ, 125, 1736

Rubin V.C., Hunter D.A., Ford W.K.Jr. 1991, ApJS, 76, 153 (R1991)

Schlegel, D., Finkbeiner, D. P., Davis, M. 1998, ApJ, 500, 525

Tully, R. B., Pierce, M. J., Huang, J. S., Saunders, W., Verheijen, M. A. W., & Witchalls, P. L. 1998, AJ, 115, 2264

Tully, R.B. & Pierce, M.J. 2000, ApJ, 533, 744

Verdes-Montenegro L., del Olmo A., Perea J., Athanassoula E., Márquez I., Augarde R., 1997, A&A, 321, 409

Verheijen M.A.W, 2001, ApJ, 563, 694

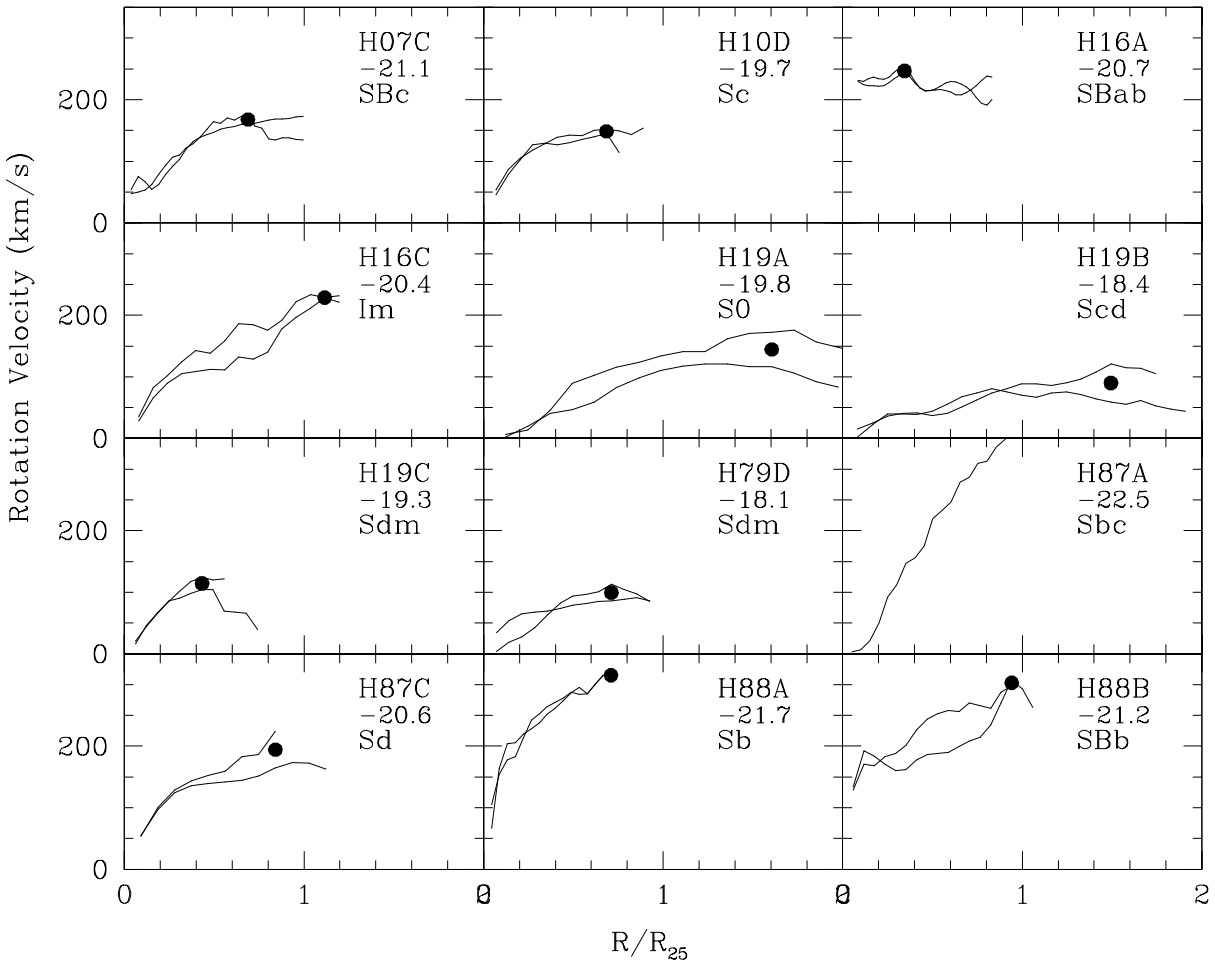

Fig. 1a.— Rotation curves for the HCG galaxies studied in this paper. The identification of the galaxies, their absolute B-magnitudes and morphological types are indicated at the top right of each subpannel. The black dots represent the maximum velocities of the average velocity curves (single averages of the values for the receding and approaching sides), values which are used in the T-F relation plotted in Fig. 4. For HCG 87a the black dot is not plotted (at V_{max} = 410 km s^{-1}) because it is off the scale.

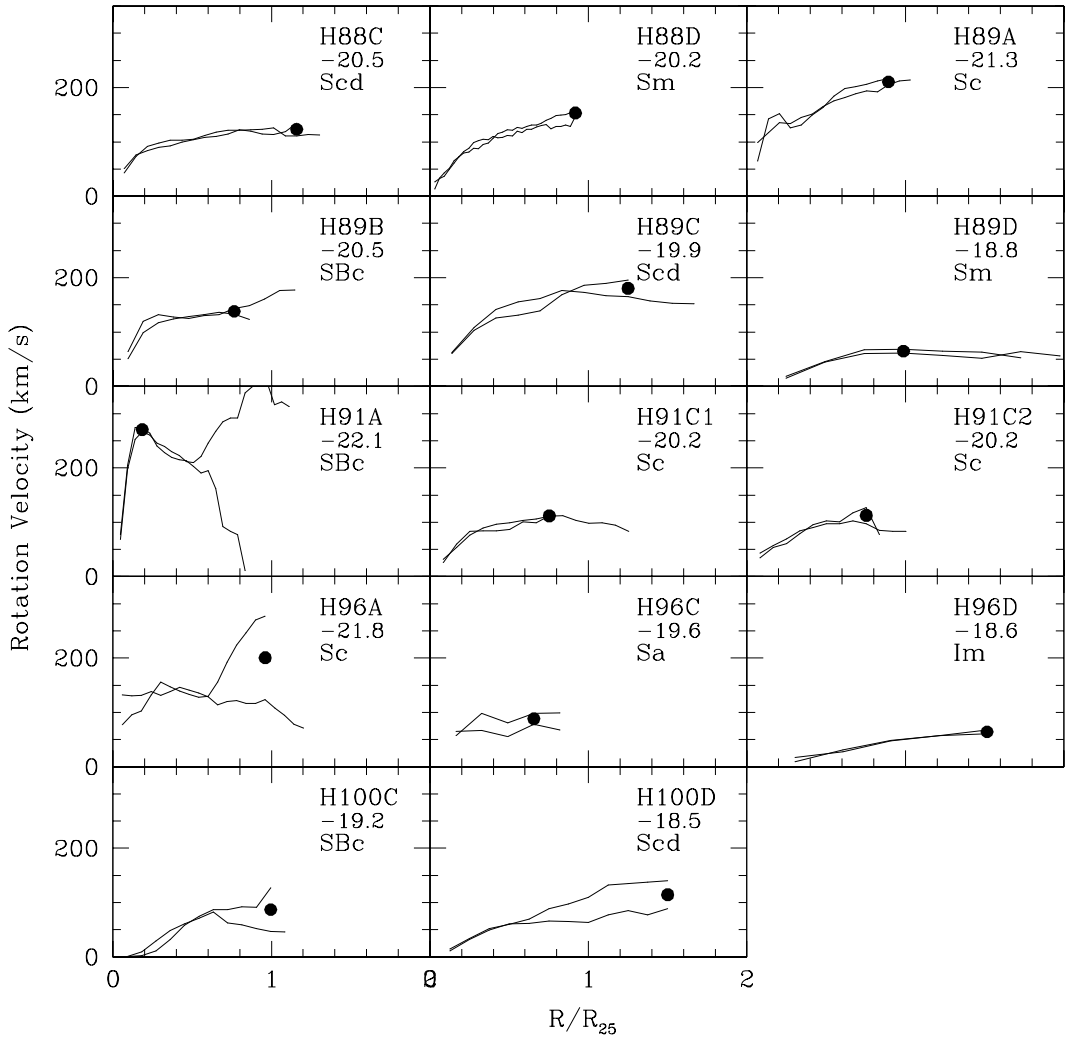

Fig. 1b.— Cont. HCG 91c has two kinematic components of similar amplitudes (C1 is the only component represented in the T-F relation of Fig. 4). Both are plotted above. Note the bifurcation in the curves of HCG 91a and HCG 96a, with one side of the curve rising and the other one falling. Interestingly, these two galaxies are the most massive members of M51-like-pairs (see section 5.3 for details).

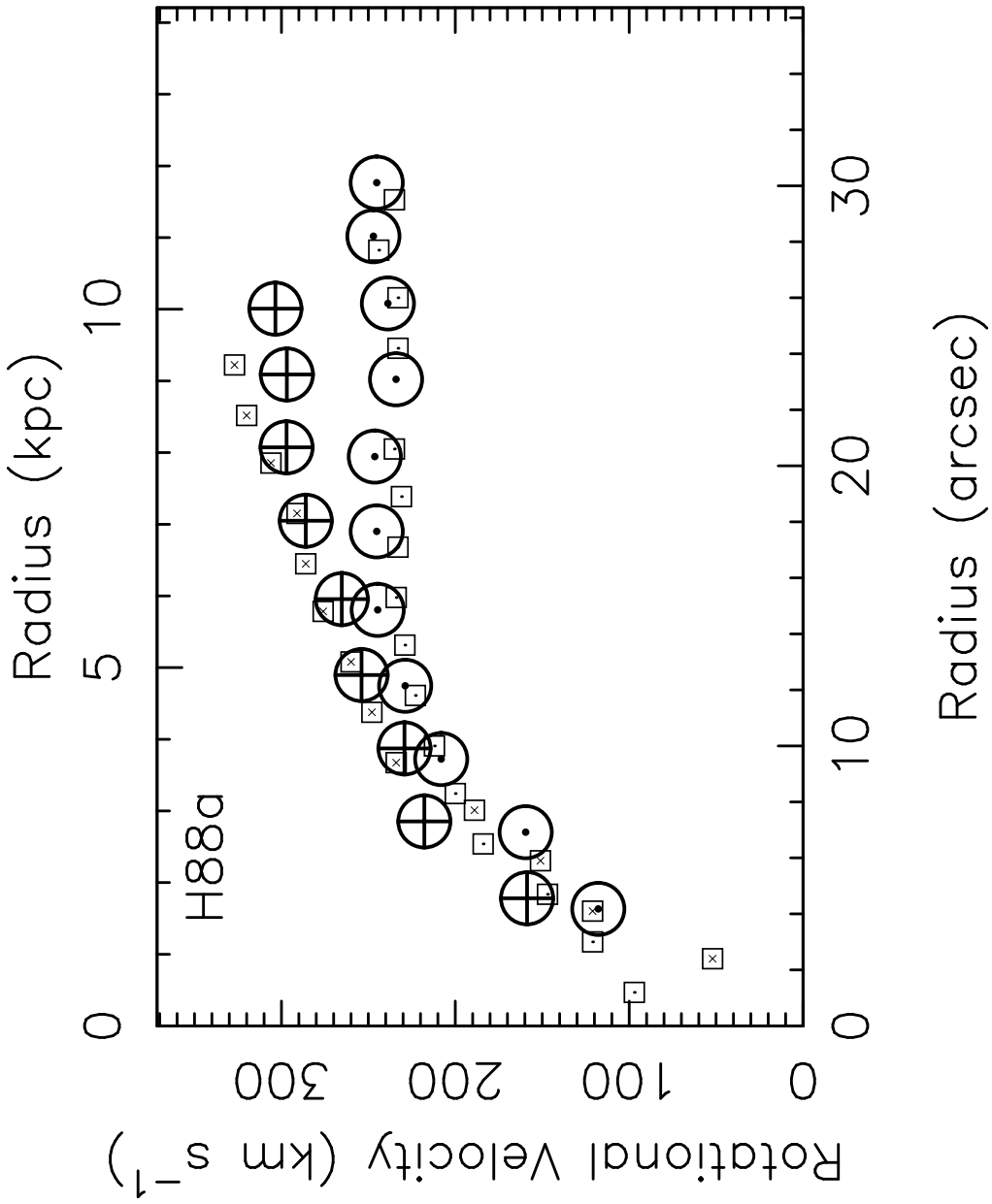

Fig. 2.— HCG 88a – Rotation curve obtained for the values of center, inclination and position angle measured by R1991, using the galaxy photometry (central velocity = 5969 km s^{-1}, inclination = 68 degrees, position angle = 127 degrees). The circles are, for each annulus, the average velocities for the receding (circled crosses) and the approaching side (circled dots), measured in the Fabry-Perot data within ± 15 degrees of the major axes in the plane of the sky (the narrow cone of 15 degrees is an attempt to mimic a long slit). The squares plot the velocity points of R1991. The squares with dots inside correspond to the receding and with X's to the approaching side of the galaxies. For radii larger than 10 arcsec, there is rather good agreement between the Fabry-Perot and slit-spectroscopy data, for these particular values of center, inclination and position angle. However, the overall shape of the curve changes when such parameters are derived from the velocity map and a large sector of the galaxy is averaged (the resulting rotation curve is shown in Plana et al. 2003 and in Fig. 1). In particular, the bifurcation present in the figure above, at r $\sim$ 10 arcsec, disappears, when the curve is plotted using the kinematic parameters and considering a large sector of the galaxy.

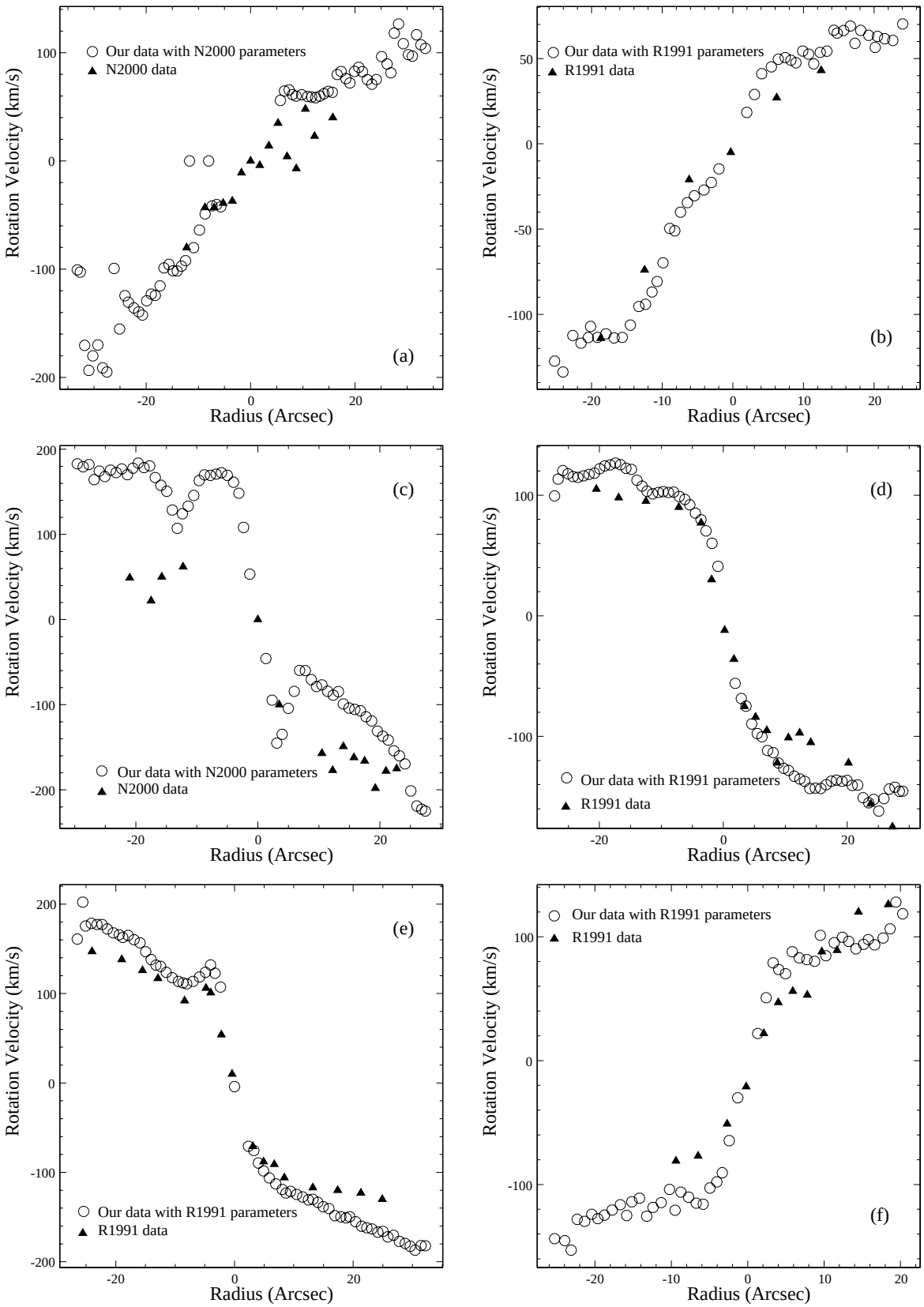

Fig. 3.— Comparison between the rotation curves derived from our data and those derived by R1991 and N2000. In all cases, in order to match the long slit data, we mimic a slit through our data using the values of inclination and PA given by the other authors. (a) HCG 79d – The data of N2000 are complementary to ours and they show the same trend. South is to the left and north is to the right of the figure. (b) HCG 79d – The agreement between R1991 and our data is within 20 kms^{-1}, but the R1991 data do not reach a plateau. (c) HCG 88b – The two datasets do not agree and our data extend further out. NE is to the left and SW is to the right. (d) HCG 88c – SE is to the left and NW is to the right. (e) HCG 89a – NE to the

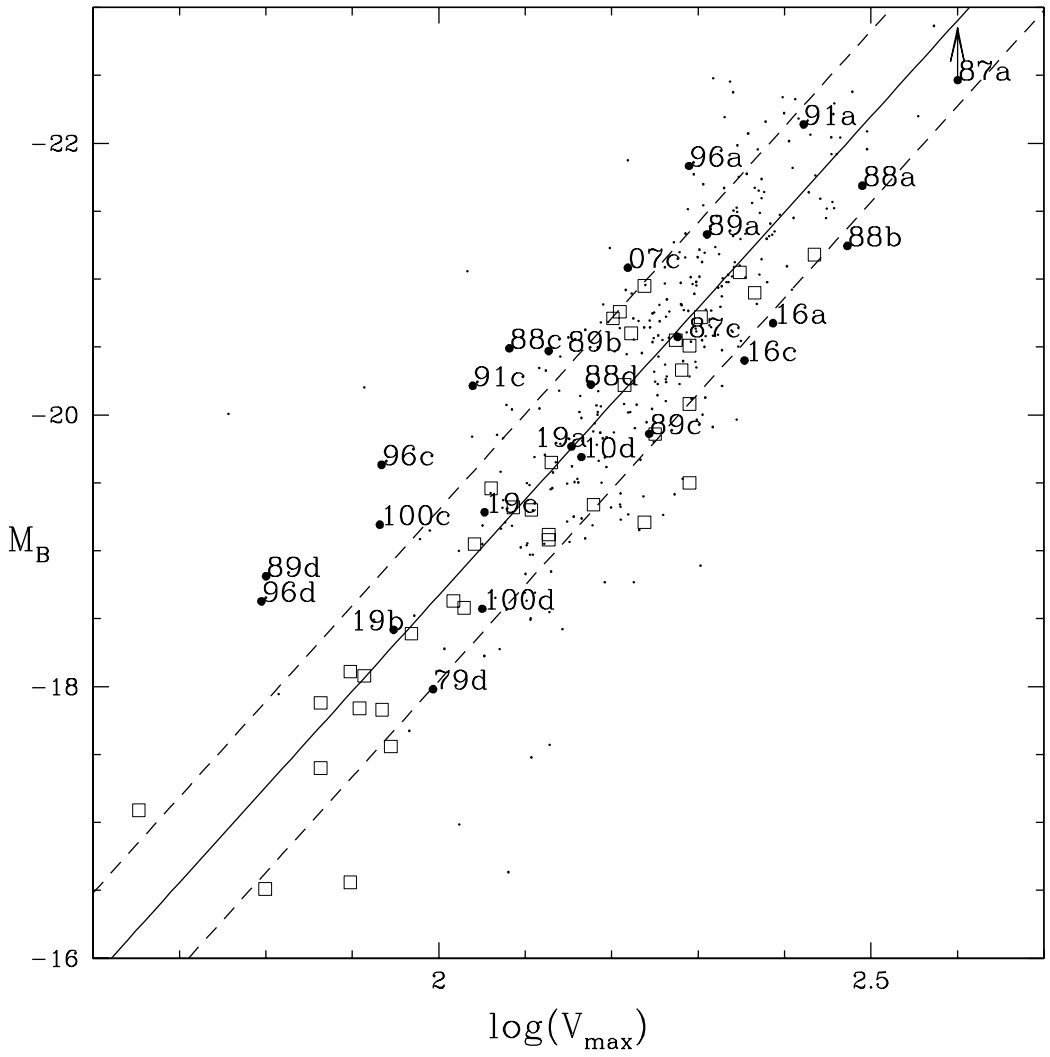

Fig. 4.— The Tully Fisher relation for samples of compact group (large black dots), field (small black dots, from Courteau's data) and Ursa Major cluster galaxies (squares, from Verheijen's data). The solid and broken lines represent the least squares fit and one-sigma dispersions for the Courteau's data respectively. HCG 87a is known to be dusty and therefore its magnitude is probably brighther than what is plotted here.

TABLE 1
MAIN PARAMETERS FOR EACH GALAXY

HCG	Size in arcsec	Morphological Type (Hickson)	Morphological Type (NED)	B_{Tcor}	V_{rot} $km\ s^{-1}$	vvir (LEDA) $km\ s^{-1}$	Absolute Magnitude	Vel. Field P=peculiar
07c	52.3	SBc	SAB(r)c	12.67	168	4369	-21.08	
10d	29.2	Sc	Scd	14.41	149	4781	-19.69	
16a	34.9	SBab	SAB(r)ab	12.82	247	3748	-20.68	
16c	31.5	Im/S0a	SA(rs)0	13.09	229	3766	-20.40	P
19a	26.2	S0	S0	13.93	144	4157	-19.77	P
19b	24.1	Scd	SB(r)a	15.28	90	4109	-18.42	P
19c	32.4	Sdm	SBm	14.41	115	4032	-19.28	
79d	28.1	Sdm	SB(s)c	15.91	100	4678	-17.98	P
87a	39.8	Sbc	S0	12.88	410	8645	-22.46	–
87c	21.4	Sd	Sb	14.78	195	8858	-20.57	P
88a	45.1	Sb	Sb	12.84	315	5972	-21.69	
88b	34.0	SBb	SB(r)a	13.28	303	6026	-21.24	P
88c	27.6	Scd	SAB(r)bc	14.04	123	6074	-20.49	
88d	32.7	Sm	Sc	14.3	153	6052	-20.22	
89a	29.1	Sc	Sc	14.04	210	8858	-21.33	P
89b	20.9	SBc	SBc	14.90	138	8950	-20.47	P
89c	14.4	Scd	Scd	15.51	180	8893	-19.86	P
89d	8.1	Sm	Sm	16.56	65	8878	-18.81	P
91a	43.2	SBc	SB(s)bc	12.71	271	6539	-22.14	P
91c	23.9	Sc	Sc	14.64	112	7185	-20.21	P
96a	33.3	Sc	SA(r)bc	13.52	201	8799	-21.83	P
96c	12.2	Sa	Sa	15.72	88	8709	-19.63	P
96d	6.6	Im/Sd	Im	16.72	64	9011	-18.63	P
100c	22.1	SBc	SBc	15.12	87	5507	-19.19	P
100d	16.0	Scd	Scd	15.74	114	5635	-18.57	P

TABLE 2

Galaxies	Our data					RHF1991 data		Nish2000 data	
(1)	i_{kin} (2)	i_{cont} (3)	PA_{kin} (4)	PA_{cont} (5)	$\|\Delta_{kin-cont}c\|$ (6)	i (7)	PA (8)	i (9)	PA (10)
HCG 07 c	48	36	133	133	0.9				
HCG 10 c	48	64	153	33	4.2				
d	68	75	147	135	1.2				
HCG 16 a	43	57	3	0	1.3	42	8		
b	72	58	70	86	2.6	64	86		
c	60	48	120	115	6	38	78		
d	47	27	70	80	0.4	60	86		
HCG 19 a	53	57	67	44	3.7				
b	60	35	90	87	5.9				
c	55	50	103	105	0.4				
HCG 79 d	58	78	170	180	0.4	80	191	90	0
HCG 87 a	85	70	52	50	1.6			90	56
c	50	60	82	90	1.2			76	90
HCG 88 a	65	55	128	126	1.2	68	127	64	132
b	55	45	160	34	3.8			43	31
c	42	...	150	...	1.2	34	160	32	31
d	70	73	70	70	2.9			90	71
HCG 89 a	45	51	54	44	0.6	60	52	51	57
b	49	65	165	155	1.2	63	141		
c	46	65	0	0	0				
d	50	45	70	87	2.5				
HCG 91 a	50	50	0	50	2.5				
c1	40	50	141	125	1.2				
c2	45	50	125	125	1.2				
HCG 96 a	50	60	132	150	1.8			25	90
c	57	53	33	33	0				
d	48	56	10	0	1.8				
HCG 100 a	50	47	78	78	1.3	60	85		
b	52	57	145	165	2.8				
c	66	65	72	70	2.5	68	73		
d	70	64	53	47	1.9				

[1] Galaxy identification. Note that HCG 10c, 16b, 16d, 100a and 100b were not included in the T-F analysis
[2] Inclination in degrees from our velocity field
[3] Inclination in degrees from our continuum map
[4] Position angle in degrees from in velocity field
[5] Position angle in degrees from in continuum map
[6] Difference between the kinematical center and the continuum center, in arsec
[7] Inclination in degrees measured by R1991
[8] PA in degrees measured by R1991
[9] Inclination in degrees measured by N2000
[10] PA in degrees measured by N2000